Solid 3D vs Plane Stress Shell Formulations of Anisotropic Non Normal Plasticity with Damage for Sheet Metal Forming

H.Badreddine[1], K. Saanouni[1]
[1] *ICD/Lasmis, University of Technology of Troyes, Troyes, France*

Abstract. In order to predict the ductile damage occurrence in metal forming, an "advanced" finite anisotropic elastoplastic constitutive equations accounting for the "strong" coupling with ductile damage have been developed and implemented in general 3D purpose F.E. software ABAQUS/Explicit®. The aim of this paper is to compare the 3D formulation using solid elements to the plane stress formulation within shell elements, regarding their ability to predict failure in sheet metal forming. Comparisons are made in term of the damage and thickness distributions as well as the global force – displacement curves. It has been shown that the plane stress assumption gives quite different results compared to the realistic 3D case when the damage effect (coupling) is taken into account. Also, the plane stress assumption is no more valid when plastic flow together with damage is highly localized.

1 INTRODUCTION

Ductile (or plastic) damage often occurs during sheet metal forming processes due to the large plastic flow and its localization in some limited zones. Accordingly, it is important to use fully coupled constitutive equations accounting for both hardening and the ductile damage when simulating numerically these processes. This will be hepfull in both cases, namely to overcome the damage initiation during some bulk and sheet metal forming processes as forging, stamping, deep drawing, ... or to enhance the damage initiation and growth as in sheet metal cutting or metal machining by chip formation for example.
In our laboratory, an extensive work has been developed since ten years, in order to describe the ductile damage modelling in sheet metal forming [1-7]. Based on the thermodynamics of irreversible processes with state variables, the advanced approach aims to model the coupling between the main mechanical fields and the ductile damage. These models have been implemented in Abaqus/standard and Abaqus/explicit using the available user subroutines (Umat and Vumat). In the present work this approach will be shortly discussed from both the theoretical and numerical point of views.
For sheet metal forming, often shell elements based on plane stress formulation are used to reduce CPU time. Some applications are made to various sheet metal forming examples. Calculations using both shell and 3D solid elements are compared with respect to the damage occurrence and the plastic flow localisation. The validation of the plane stress assumption becomes highly questionable when localization takes place inside the sheet.

2 FULLY COUPLED CONSTITUTIVE EQUATIONS OF NON NORMAL ANISOTROPIC PLASTIC MODEL COUPLED WITH DUCTILE DAMAGE

Assuming that in metal forming, by large plastic deformation, the elastic part of the total strain remains infinitesimal compared to the plastic one, the total strain rate decomposes additionally as:

$$\underline{D} = \underline{\dot{\varepsilon}}^{e}_{J} + \underline{D}^{p} \tag{1}$$

where the first term represents the Zaremba_Jaumann objective derivatives of the small elastic strain and the second represents the finite plastic (objective) strain rate defined thanks to the appropriated dissipation potential (see later). On the other hand, the objectivity requirement is satisfied by using the so called rotating frame formulation (RFF) (see [9, 10] among many others). This aims to formulate the constitutive equations on an appropriated intermediate configuration having the same Lagrangian orientation as the initial undeformed configuration. This consists to rephrase any constitutive model developed under the small strain hypothesis by replacing any tensor $\overline{\underline{T}}$ by its corresponding one

$$\overline{\underline{T}} = \underline{\underline{Q}}^{T}\,\underline{T}\,\underline{\underline{Q}} \tag{2}$$

rotated by the orthogonal rotation tensor $\underline{\underline{Q}}$ itself solution of the following 'kinematical' constitutive equation:

$$\dot{\underline{\underline{Q}}}.\underline{\underline{Q}}^{T} = \underline{W} \text{ with } \underline{\underline{Q}}(t=0) = \underline{\underline{Q}}^{0} \tag{3}$$

$\underline{W}$ is the spin rate of the rotated frame [9-11]. This rotated description keeps unchanged the basic structure of the constitutive equations as formulated in small strain hypothesis.

Using this 'rotated' objective formulation a complete set of constitutive equations can be formulated for metal forming simulation. In this paper the non associative and non normal anisotropic plastic formulation accounting for the nonlinear isotropic (r, R) and kinematic $\left(\overline{\underline{\alpha}}, \overline{\underline{X}}\right)$ hardening fully coupled with the isotropic damage (d, Y) under isothermal condition is considered (see [7] for the general anisotropic and anisothermal formulation). The outline of this model is given here after when all the tensorial quantities with a bar ($\bar{}$) refer to the rotated configuration as discussed above (see Eq.2):

*the stress-like state variables:

Cauchy stress tensor: $$\overline{\underline{\sigma}} = (1-d)\,\overline{\underline{\underline{\Lambda}}} : \overline{\underline{\varepsilon}}^{e} \tag{4}$$

Back stress tensor: $$\overline{\underline{X}} = \frac{2}{3}(1-d)\,C\,\overline{\underline{\alpha}} \tag{5}$$

Isotropic hardening stress $$R = (1-d)\,Q\,r \tag{6}$$

Damage stress $$Y = \frac{1}{2}\bar{\underline{\varepsilon}}^{e} : \bar{\underline{\underline{\Lambda}}} : \bar{\underline{\varepsilon}}^{e} + \frac{1}{3} C\, \bar{\underline{\alpha}} : \bar{\underline{\alpha}} + \frac{1}{2} Q\, r^2 \tag{7}$$

where $\bar{\underline{\underline{\Lambda}}}$ is the symmetric and positive definite fourth order elastic properties tensor of the non damaged material which in the isotropic case takes the well known form: $2\mu^e \underline{\underline{I}} + \lambda^e \underline{1} \otimes \underline{1}$. C is the kinematic hardening modulus and Q is the linear isotropic hardening modulus.

* the evolution (or constitutive) equations:

$$\bar{\underline{D}}^{p} = \frac{\dot{\lambda}}{\sqrt{1-d}} \bar{\underline{n}}^{p}, \quad \bar{\underline{n}}^{p} = \frac{\partial \sigma^{p}}{\partial \bar{\underline{\sigma}}} = \frac{\bar{\underline{\underline{H}}} : \left(\bar{\underline{\sigma}} - \bar{\underline{X}} \right)}{\sigma^{p}} \tag{8}$$

$$\dot{\bar{\underline{\alpha}}} = \dot{\lambda} \left[\frac{1}{\sqrt{1-d}} \bar{\underline{n}}^{p} - a\, \bar{\underline{\alpha}} \right] \tag{9}$$

$$\dot{r} = \dot{\lambda} \left[\frac{1}{\sqrt{1-d}} - b r \right] \tag{10}$$

$$\dot{d} = \dot{\lambda} \frac{1}{(1-d)^{\beta}} \left\langle \frac{Y - Y_0}{S} \right\rangle^{s} \tag{11}$$

where $\dot{\lambda}$ is the plastic multiplier which is determined by the consistency condition applied to the yield function :

$$\dot{\lambda} = \begin{cases} \left\langle \frac{1}{H^{p}} \bar{\underline{a}}^{p} : \bar{\underline{D}} \right\rangle & \text{if} \quad f = \dot{f} = 0 \\ 0 & \text{otherwise} \end{cases} \tag{12}$$

Where

$$\bar{\underline{a}}^{p} = \sqrt{1-d}\; \bar{\underline{\underline{\Lambda}}} : \bar{\underline{n}}^{c}, \quad \bar{\underline{n}}^{c} = \frac{\partial \sigma^{c}}{\partial \bar{\underline{\sigma}}} = \frac{\bar{\underline{\underline{H}}} : \left(\bar{\underline{\sigma}} - \bar{\underline{X}} \right)}{\sigma^{c}} \tag{13}$$

$$\begin{aligned} H^{p} = {} & \bar{\underline{n}}^{c} : \left(\bar{\underline{\underline{\Lambda}}} + \frac{2}{3} C \underline{\underline{I}} \right) : \bar{\underline{n}}^{p} - \frac{a}{\sqrt{1-d}} \bar{\underline{n}}^{c} : \bar{\underline{X}} + Q \\ & - \frac{bR}{\sqrt{1-d}} + \frac{\sigma_y}{2} \frac{1}{(1-d)^{\beta+1}} \left\langle \frac{Y - Y_0}{S} \right\rangle^{s} \end{aligned} \tag{14}$$

The plastic yield function f is given by:

$$\bar{f} = \frac{\sigma^{c}(\bar{\underline{\sigma}} - \bar{\underline{X}})}{\sqrt{1-d}} - \frac{R}{\sqrt{1-d}} - \sigma_y \leq 0 \tag{15}$$

Where σ_y is the initial yield stress in simple tension; a and b characterize respectively the kinematic and isotropic hardening non linearity; β, S, s and Y_0 characterize the ductile damage evolution.

The stress norms σ^p and σ^c are the equivalent stresses entering the yield and the plastic potential functions. They can be chosen as quadratic [19] or non quadratic functions of the effective stress $\left(\overline{\underline{\sigma}} - \overline{\underline{X}}\right)$. In the present work both σ^p and σ^c are taken as quadratic functions of the Hill 1948 type:

$$\bar{\sigma}^{\,c} = \sqrt{\left(\overline{\underline{\sigma}} - \overline{\underline{X}}\right) : \overline{\underline{\underline{H}}} : \left(\overline{\underline{\sigma}} - \overline{\underline{X}}\right)} \tag{16}$$

$$\bar{\sigma}^{p} = \sqrt{\left(\overline{\underline{\sigma}} - \overline{\underline{X}}\right) : \overline{\underline{\underline{H}}}' : \left(\overline{\underline{\sigma}} - \overline{\underline{X}}\right)} \tag{17}$$

where $\overline{\underline{\underline{H}}}$ (resp. $\overline{\underline{\underline{H}}}'$) is the well known positive definite and symmetric fourth order tensor of the plastic yield function (resp. of the plastic potential) characterized by six material constants F, G, H, L, M and N (resp. F', G', H', L', M', N'). Note that the classical normal and non associative plasticity is recovered by taking $\overline{\underline{\underline{H}}} = \overline{\underline{\underline{H}}}'$ leading to $\sigma^c = \sigma^p$.

3 NUMERICAL ASPECTS

The model developed above has been implemented into ABAQUS/Explicit® FE software for metal forming simulation thanks to the user subroutine Vumat (ABAQUS® Theory Manual). The dynamic explicit global resolution scheme is developed in detail in (ABAQUS® Theory Manual) considering the contact with friction of Coulomb type characterized by the friction parameter η. The computation of the stress tensor $\overline{\underline{\sigma}}$ on the rotated (Lagrangian) configuration is required in order to evaluate the internal stress vector at each integration point inside each finite element and for the end of each time increment. This is realized by integrating all the constitutive equations of the model presented above including the ductile damage. The classical incremental and iterative elastic predictor – plastic corrector method [12] is used. This approach consists of applying a total strain step $\Delta\underline{\varepsilon}$ taken from the transformation gradient increment $\Delta\underline{F}$ at every time increment $[t_n , t_{n+1}]$ with $t_{n+1} = t_n + \Delta t$. At the beginning of a given increment all the fields ($\overline{\underline{\sigma}}_n$, $\overline{\underline{\varepsilon}}^p_n$, $\overline{\underline{X}}_n$, $\overline{\underline{Q}}_n$, R_n, d_n) are supposed to be known and the problem is to compute their values so that the yield criterion eq.(15) should be identically zero at the end of the time increment t_{n+1}. An elastically predicted stress $\overline{\underline{\sigma}}^{trial}_{n+1}$ is calculated by supposing that the loading increment $\Delta\underline{\varepsilon}$ is purely elastic and the internal variables remain at their values at t_n. If the corresponding yield function is higher than zero (i.e;

$f(\overline{\underline{\sigma}}_{n+1}^{trial}, \overline{\underline{X}}_n, R_n, d_n) > 0$) a plastic correction is worked out on the stress and the other state variables in the manner that the yield criterion remains verified at the end of the time increment. The backward Euler and the asymptotic [14] schemes are used with reducing the number of equations to be integrated from 21 to only 8 scalar equations of the three unknowns $\overline{\underline{n}}_{n+1}^{p}$, $\Delta\lambda$ and d_{n+1} given by (see [4-7]) in the general 3D case:

$$\begin{cases} \underline{\overline{h}}_{n+1} = \overline{\underline{n}}_{n+1}^{p} - \dfrac{\overline{\overline{\overline{H}}}' : \left[\overline{\underline{\sigma}}_{n+1} - \overline{\underline{X}}_{n+1}\right]}{\sigma_{n+1}^{p}} = \underline{0} \\ f_{n+1} = \overline{\sigma}_{n+1}^{c} - R_{n+1} - \sqrt{1-d_{n+1}}\,\sigma_y = 0 \\ g_{n+1} = d_{n+1} - d_n - \Delta\lambda \hat{Y}_{n+1} = 0 \end{cases} \qquad (18)$$

where, for simplicity, use has been made of the notation $\hat{Y}_{n+1} = \dfrac{1}{(1-d_{n+1})^{\beta}} \left\langle \dfrac{Y_{n+1} - Y_0}{S} \right\rangle^{s}$.

To assume the plane stress formulation we introduce the condition $\left(\overline{\underline{\sigma}}_{n+1}\right)_{33} = 0$. This condition imposes that the strain increment $\Delta\varepsilon_{33}$ will be calculated from the local behaviour equations and not deduced from the kinematics. Accordingly, an additional equation has to be solved with the equations (eq.18) and a 4th unknown $\Delta\varepsilon_{33}$ is added. This additional equation writes:

$$k_{n+1} = \frac{1-d_{n+1}}{1-d_n}\left(\overline{\underline{\sigma}}_{n+1}^{trial}(\Delta\varepsilon_{33})\right)_{33} - 2.\mu^{e}.\Delta\lambda.\sqrt{1-d_{n+1}}\left(\overline{\underline{n}}_{n+1}^{p}\right)_{33} = 0 \qquad (19)$$

For the 3D problems only the eq.18 are solved, however for the shell structures both eq.18 and eq.19 are solved. The iterative resolution scheme is performed thanks to classical Newton-Raphson method in order to obtain, at convergence, the values of the unknowns $\overline{\underline{n}}_{n+1}^{p}$, $\Delta\lambda$, d_{n+1} and $\Delta\varepsilon_{33}$ from which all the other state variables can be easily obtained.

Tableau 1. Values of the model parameters for the used material.

parameter	E	ν	σ_y	F	G	H	L	M	N
unit	MPa	-	MPa	-	-	-	-	-	-
	195000	0.3	405	0.9	0.6	0.4	1.500	1.500	2.8
parameter	F'	G'	H'	L'	M'	N'	Q	b	C
unit	-	-	-	-	-	-	MPa	-	MPa
	0.2	0.4	0.6	1.500	1.500	1..0	5500	10.0	38000
parameter	a	s	S	β	Y_0				
unit	-	-	MPa	-	MPa				
	290	1	45	2	0				

4 APPLICATIONS

Some examples of sheet metal forming are now simulated with the proposed model using the material constants given in Table 1. The material anisotropic parameters are chosen in the manner to give arbitrary very high anisotropy for both the yield stress criterion and the plastic flow rule (see (Fig.1)). All the examples are made using both the volume 3D elements (C3D8R) and thin shell (S4R) elements from ABAQUS® element library.

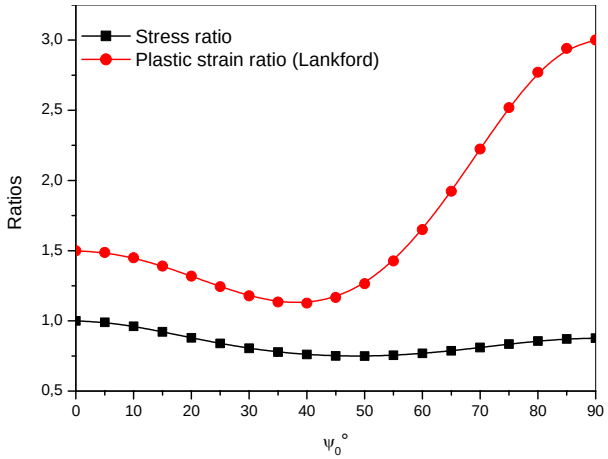

Fig 1. Stress ratio and Lankford coefficient of the considered high anisotropy.

4.1 Cylindrical deep drawing cup test

This example concerns the well known Swift deep drawing test. For the plane stress calculation the blank sheet is meshed with 12000 S4R shell elements (with 3 gauss point in the element thickness) and for the general 3D calculation the blank is meshed with 36000 elements (3 element layers in the thickness direction). The (Fig.2) shows comparison of damage maps obtained with 3D and shell elements for two different punch displacements. In this figure we can observe that maximum damaged areas are the same, but the displacement of the first damage initiation is quite different. In (Fig.3b) we observe that the punch force-displacement curves are closed until the softening stage. Note that the maximum punch force due to the 3D model is about 17% higher than the shell elements calculations. In (Fig.3a) we observe that the thickness reduction follows the damage distribution. However, the 3D solid calculation gives more important thickness reduction with less damage values. The calculation CPU times are about 8 hours with shell elements and 21 hours for 3D solid elements (3 times more important).

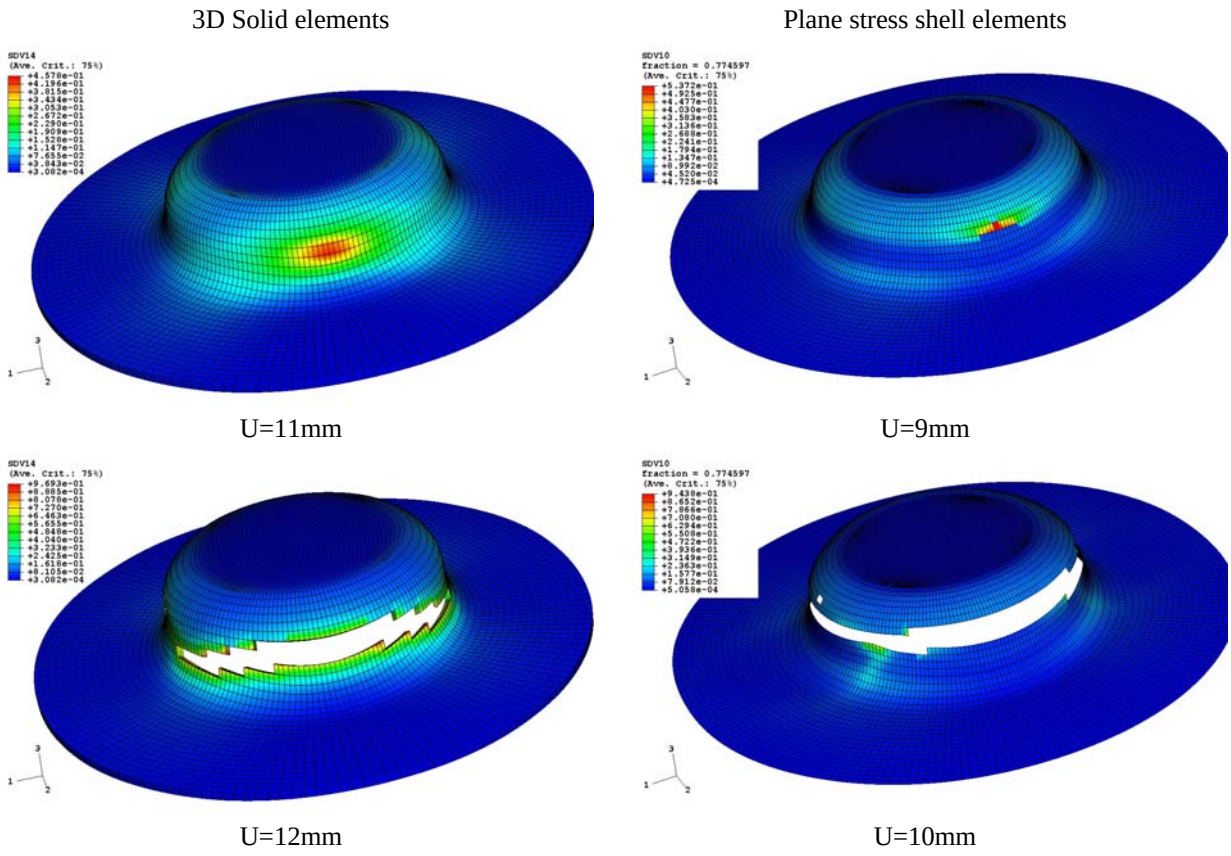

Fig 2. Damage maps of the swift test for different punch displacement obtained with 3D solid elements and thin shell elements (upper face).

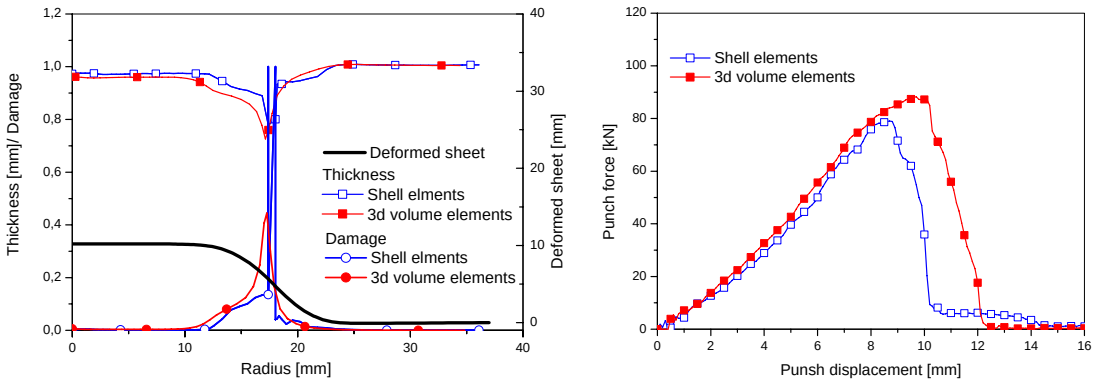

(a) Damage and thickness distributions along meridian path for u=11mm.

(b) Global punch force –displacement curves.

Fig 3. Comparisons of global and local results obtained with 3D solid elements and thin shell elements (3 gauss points).

4.2 Cross deep drawing test

This example concerns the widely used cross deep drawing test. For the plane stress calculation the blank sheet is meshed with 15000 S4R shell element (with 5 gauss points) and for the general 3D calculation the blank is meshed with 60000 elements (4 element layers in the thickness direction). The (Fig.4) shows a comparison of damage maps obtained with 3D and shell elements for two different punch displacements. In this figure we can observe, as the previous example, that maximum damaged zones are the same, but the location of the first "crack" initiation is quite different. In (Fig.5) we observe that the punch force-displacement curves are quite similar until the softening stage. We remark that the maximum punch force due to the 3D solid elements is about 15% higher. Concerning the CPU times, we have obtained about 12 hours with shell elements and 34 hours for 3D solid elements (3 times more important).

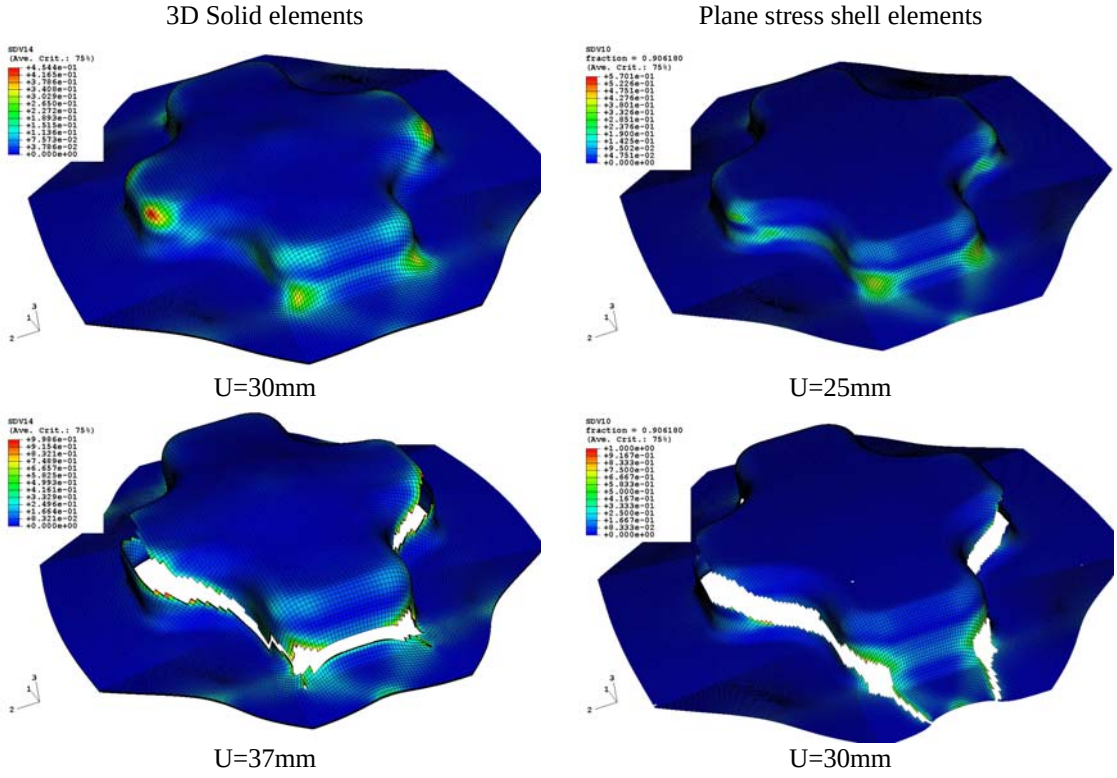

Fig 4. Damage maps of the cross deep drawing test for different punch displacements obtained with 3D solid elements and thin shell elements.

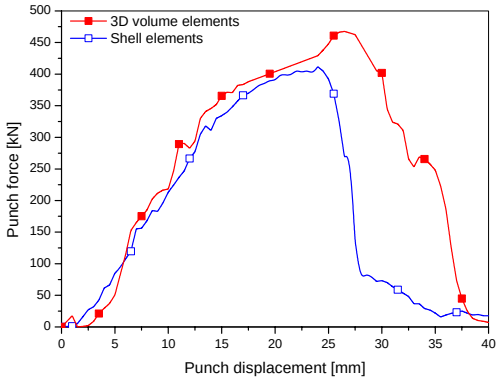

Fig 5. Global punch force –displacement curves of the cross test.

5 CONCLUSION

In this paper theoretical formulation and numerical implementation of a finite deformations anisotropic elastoplastic model fully coupled with isotropic ductile damage is shortly presented. General 3D and plane stress cases of the model are compared through some sheet metal forming examples. The simulations reveal that with the damage occurrence the general 3D gives quite different results compared to plane stress ones. Despite a more important CPU time, the general 3D case is more realistic because it takes into account more accurately the mechanical fields gradients through the thickness. This is very important also to predict damage localization through the sheet thickness. However, the plane stress assumption becomes no longer valid after the localization takes place.

References

[1] Saanouni K., Hammi Y., « Numerical simulation of damage in metal forming processes », in Continuous Damage and Fracture , Editor A. Benallal, Elsevier, ISBN. 2-84299-247-4, pp :353-363, 2000

[2] Saanouni K., Cherouat A. and Hammi Y., «Numerical aspects of finite elastoplasticity with isotropic ductile damage for metal forming», Revue Européenne des Eléments Finis, 2-3-4, pp. 327-351, 2001

[3] Saanouni, K., Forster C. and Ben Hatira F., « On the Anelastic Flow with Damage », Int. J. Dam. Mech., 3:140-169, 1994

[4] Khelifa M., Badreddine H., Belamri N., Gahbich M. A., Saanouni K., Cherouat A., Dogui A., Effect of anisotropic plastic flow on the ductile damage evolution in hydrobulging test of thin sheet metal, Int. Journal of Forming Processes, Vol. 8, N°:2, pp : 271-289, 2005

[5] Khelifa M., K., Saanouni, H., Badreddine, M.-A., Gahbiche, and A., Dogui, "Plasticité anisotrope couplée à un endommagement ductile isotrope: Appliction au gonflement hydraulique de tôles minces", Revue Européenne des Eléments Finis, Vol15., N°7-8, pp. 891-908, 2006.

[6] Badreddine H., Saanouni K., Dogui A., Gahbich M.A., Elastoplasticité anisotrope non normale en grandes déformations avec endommagement. Application à la mise en forme de tôles minces. Revue Européenne de Mécanique Numérique, Vol. 15, N°7-8, 2006,pp :891-908.

[7] Saanouni K. and Chaboche J.L., 'Computational Damage Mechanics. Application to Metal Forming', Chapter 7 of the Volume 3 : 'Numerical and Computational methods' (Editors: R. de Borst, H. A. Mang), in 'Comprehencive Structural Integrity', Edited by I. Milne, R.O. Ritchie and B. Karihaloo, ISBN: 0-08-043749-4, 2003, Elsevier, Oxford

[8] Hambli R., «Finite element model fracture prediction during sheet-metal blanking processes», Eng. Fracture Mechanics, 68, pp.365-378, 2001

[9] Dogui, A.., "Plasticité anisotrope en grandes déformations", Thèse de doctorat d'état, Université Claude Bernard, lyon I, 1989

[10] F., Sidoroff and A., Dogui, « Some issues about anisotropic elastic-plastic models at finite strain », Int. J. Sol. Str. 38, 2001, 9569-9578.

[11] Simo J.C., Hughes T.J.R., Computational inelasticity, Springer, New York, 1998

[12] J.C. Simo, and M., Ortiz, « A Unified Approach to Finite Element Deformation Elastoplastic Analysis Based on the Use of Hyperelastic Equations », Comp. Meth. Appl. Meth. Engng., vol 49, 1985, pp, 221-245.

[13] T. J. R., Hughes, J., Winget, « Finite rotation effects in numerical integration of rate constitutive equations arising in large-deformation analysis », Int. J. Nume. Meth. Engng, 15, 1980: 1862-1867.

[14] D. Freed, and K. P., Walker, «Exponential integration algorithm for first-order ODEs with application to viscoplasticity». ASME Summer Conf. On Mechanics and Materials Recent Advances on Damage Mechanics and Plasticity, Tempe, 1992.

[15] Belytschko, T., Liu, W.K. and Moran, B., Nonlinear finite elements for continua and structures, John Wiley, New York, 2000

[16] Villon P., Borouchaki H., Saanouni K., Transfert de champs plastiquement admissibles. CRAS, Mécanique, 330 (2002), pp :313-318

[17] Lemaitre, J., and Chaboche J.L., Mécanique des Matériaux Solides, Dunod, Paris, 1985.

[18] Lemaitre, J. , A Course of Damage Mechanics, Springer Verlag, Heidelberg, 1992.

[19] Hill R., « A theory of yielding and plastic flow of anisotropic metals », Royal Soc, London Proc. p. 281, 1948.